

# Self-assembly of long-chain quaternary ammonium cations in a hybrid inorganic–organic material with one-dimensional polymeric tribromidoplumbate(II)

Maciej A. Hodorowicz,\* Agata Piaskowska and Katarzyna M. Stadnicka

Faculty of Chemistry, Jagiellonian University, Ingardena 3, 30-060 Kraków, Poland  
Correspondence e-mail: hodorowm@chemia.uj.edu.pl

Received 10 May 2012

Accepted 21 May 2012

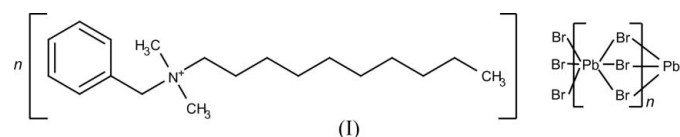
Online 13 June 2012

*catena*-Poly[benzyldecyldimethylammonium [plumbate(II)-tri- $\mu$ -bromido]],  $\{(\text{C}_{19}\text{H}_{34}\text{N})[\text{PbBr}_3]\}_n$ , crystallizes as an inorganic–organic hybrid following monoclinic space-group symmetry  $P2_1/c$ . The structure consists of extended chains running along the [001] direction and built of  $[\text{PbBr}_3]^-$  units. These inorganic chains are separated by interdigitated ammonium cations which form hydrophilic layers through weak  $\text{C}-\text{H}\cdots\text{Br}$  interactions. The architecture is essentially the same as found for *n*-alkylbenzyldecyldimethylammonium bromides.

## Comment

A persistent problem in solid-state inorganic chemistry is the correlation of structural features, characteristic for a particular type of materials, with their physical properties. In this connection, low-dimensional compounds play an important role, because the interactions between atoms and molecules, when confined to one or two dimensions, make theoretical models much simpler (Day, 1983). Many useful physical and chemical properties could only be found and defined in terms of low-dimensional structural models. For example, the architecture of alternate hydrophobic and hydrophilic layers, as observed in the crystals of alkylbenzylammonium bromides (Hodorowicz *et al.*, 2005), provided an explanation of the structure of ammonium cation layers formed at the surface or intercalated between the silicate units, such as those observed in Na–montmorillonite (Kwolek *et al.*, 2003). This knowledge could be utilized in the crystal engineering of organoclays for specific applications. On the other hand, halometalates(II) represent particularly suitable systems for designing the construction of low-dimensional structural archetypes from which modifications with enhanced properties could be derived. The synthesis of inorganic–organic hybrids based on

*n*-alkylbenzyldecyldimethylammonium cations and inorganic  $\{[\text{PbBr}_3]^- \}_n$  chains represents an attempt to combine the properties of organic and inorganic domains to modify the macroscopic properties of the crystalline phase (Mitzi *et al.*, 2001; Portier *et al.*, 2001). Some low-dimensional polymeric halometalates of copper(II), manganese(II) and cadmium(II) have been studied previously (Ravindran *et al.*, 1990, and references therein; Bonamartini-Corradi *et al.*, 1993, 1994). Also, tin derivatives have been exploited due to their nonmagnetic semiconducting properties (Willett, 1991). Concerning haloplumbates, much work has been carried out on iodidoplumbates(II) of the  $AM_2X_{2z+1}$  type ( $A$  is an organic ammonium cation,  $M$  is a divalent metal and  $X$  is Cl, Br or I) due to their potential semiconducting properties (quantum-wire systems) (Papavassiliou, 1997). Among these systems, containing  $MX_6$  face-sharing octahedra, there are compounds like  $[\text{Et}_4\text{NPbI}_3]_n$  and  $[\text{Bu}_4\text{NPbI}_3]_n$  with short-chain quaternary ammonium cations (Papavassiliou, 1997). A few years ago, the structures of the inorganic–organic hybrids  $\{\text{Bu}_2[\text{PbI}_3]\text{I}\cdot 2\text{H}_2\text{O}\}_n$  (Billing & Lemmerer, 2006) and  $\{[(\text{CH}_3)_2\text{C}=\text{NH}-\text{CH}_2\text{CH}_2\text{CH}_3][\text{PbI}_3]\}_n$  (Elleuch *et al.*, 2007) were reported. The composition and structure of iodidoplumbate anions (chains, ribbons or rods) are determined by the size, shape and charge of the counter-ions used for crystallization (Krautscheid *et al.*, 2001). Much less is known about bromidoplumbate(II) systems with long-chain organic ammonium molecules. In the present paper, we report the structure of the inorganic–organic hybrid complex salt, (I), containing one-dimensional polymeric tribromidoplumbate(II) anions built from face-sharing  $\{\text{PbBr}_6\}$  (distorted) octahedra and quaternary benzyldecyldimethylammonium cations. The aim of this work



was to increase our knowledge of the factors controlling the stereochemistry of bromidoplumbates(II) (how the  $\text{C}-\text{H}\cdots\pi$  interactions of ammonium cations stabilize the bilayers) and the mutual packing properties of long-chain quaternary ammonium cations in different environments, particularly in relation to their behaviour in crystalline bromides (Hodorowicz *et al.*, 2005).

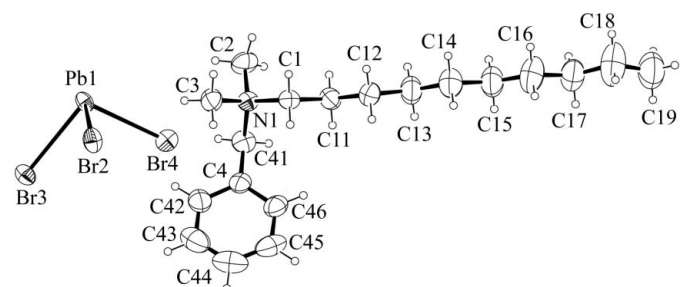
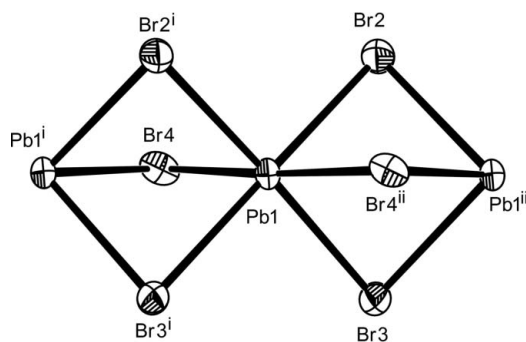


Figure 1

A view of the asymmetric unit of (I), showing the atomic numbering scheme. Displacement ellipsoids are shown at the 30% probability level.

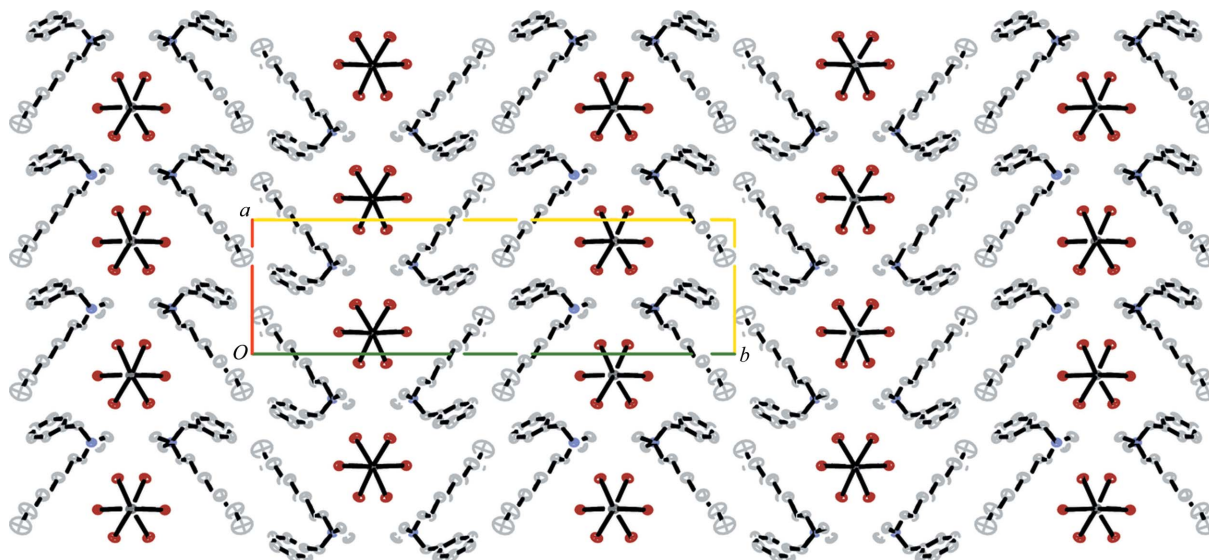

**Figure 2**

The geometry of the  $\{[\text{PbBr}_3]^{-}\}_n$  chain extended along  $[001]$ . Displacement ellipsoids are shown at the 30% probability level. [Symmetry codes: (i)  $x, -y + \frac{3}{2}, z - \frac{1}{2}$ ; (ii)  $x, -y + \frac{3}{2}, z + \frac{1}{2}$ .]

The title compound belongs to a family of one-dimensional inorganic–organic hybrid solids with the general formula  $AMX_3$ , in which  $A$  is an organic ammonium cation,  $M$  is a divalent metal, in our case  $\text{Pb}^{\text{II}}$ , and  $X$  is Cl, Br or I (Cheetham *et al.*, 2006). The structure consists of long-chain benzyldecyldimethylammonium cations and  $\{[\text{PbBr}_3]^{-}\}_n$  polymeric chains as counter-ions. The asymmetric part of the unit cell contains the ammonium cation and a  $[\text{PbBr}_3]^{-}$  unit (Fig. 1). The displacement parameters of the atoms in the decyl chain clearly increase along the chain and the highest displacements were observed for the terminal C atoms, which have additional degrees of freedom. This and some unusually short C–C bonds in some parts of the chain (Table 1) are a consequence of complex unmodelled disorder in the chain. The curvature of the hydrocarbon chain is not as severe as observed in analogous bromides (Hodorowicz *et al.*, 2005). Each  $\text{Pb}^{\text{II}}$  atom is surrounded in the one-dimensional polymeric chain by six bridging Br atoms, three of which are crystallographically independent. The polymeric chain runs along the  $c$  axis. The Pb–Br bond lengths [2.9420 (7)–3.1323 (7) Å; Table 1], agree well with those observed for other haloplumbates(II), for

example,  $[\text{PbBr}_3]^{-}$  and  $[\text{PbI}_3]^{-}$  (Nagapetyan *et al.*, 1988). All the Pb–Br bond lengths are shorter than the sum of the ionic radii ( $\text{Pb}^{2+} = 1.19$  Å and  $\text{Br}^{-} = 1.96$  Å; Shannon, 1976), probably due to partially covalent interactions. The Pb–Br bond lengths and Br–Pb–Br angles differ significantly from regular octahedral values. As a consequence, the  $\{[\text{PbBr}_3]^{-}\}_n$  unit has barely  $C_1$  symmetry, with the triangular bromide faces (Br2, Br3 and Br4) shared by two adjacent polyhedra (Fig. 2). The nonbonding intramolecular Pb $\cdots$ Pb distances are 3.8437 (2) Å. The Pb1<sup>i</sup>–Pb1–Pb1<sup>ii</sup> angle of 179.48 (1)° [symmetry codes: (i)  $x, -y + \frac{3}{2}, z - \frac{1}{2}$ ; (ii)  $x, -y + \frac{3}{2}, z + \frac{1}{2}$ ] indicates a linear development of the one-dimensional polymeric chains. Figs. 3 and 4 show the alternating hydrophilic and hydrophobic layers viewed along  $[001]$  and  $[100]$ , respectively. In Fig. 3, the mode of mutual packing of the polymeric  $\{[\text{PbBr}_3]^{-}\}_n$  chains and the benzyldecyldimethylammonium cations is presented. The polymeric  $\{[\text{PbBr}_3]^{-}\}_n$  chains parallel to  $[001]$  and the  $>\text{N}^+(\text{CH}_3)_2$  moieties of the quaternary ammonium cations form hydrophilic layers through weak C–H $\cdots$ Br interactions (geometry given in Table 2). The hydrophobic layers are composed of the benzyl and decyl groups of the ammonium cations, the mutual arrangement of which are defined by the torsion angles N1–C4–C41–C46, C1–N1–C4–C41 and C11–C1–N1–C4 (Table 1), indicating synclinal/synclinal/synclinal conformations, respectively. The decyl group has a zigzag (all *trans*) conformation. In the layers, the decyl chains are antiparallel to one another and are joined *via* weak C–H $\cdots$  $\pi$  interactions belonging to category I of the Malone weak-hydrogen-bond classification (Malone *et al.*, 1997). The C–H $\cdots$  $\pi$  interactions (Fig. 5) are responsible for the self-assembly of ammonium cations in the hydrophobic layers (Table 2).

In conclusion, an organic–inorganic layered hybrid material based on benzyldecyldimethylammonium cations, which interact with adjacent  $\{[\text{PbBr}_3]^{-}\}_n$  inorganic chains, has been obtained and structurally characterized. Due to a hydrophobic


**Figure 3**

The crystal packing, viewed along  $[001]$ , showing the layered architecture of ammonium cations and polymeric  $\{[\text{PbBr}_3]^{-}\}_n$  chains running along  $[100]$ . H atoms have been omitted for clarity. Displacement ellipsoids are shown at the 30% probability level.

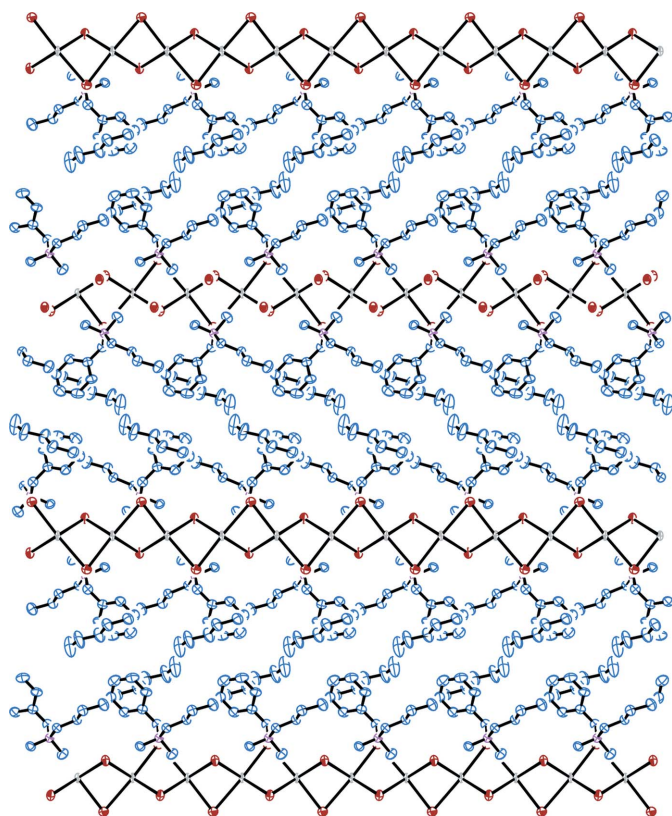


**Figure 4**  
Projection along [001] clearly emphasizing the organic–inorganic hybrid nature of the material. Displacement ellipsoids are shown at the 30% probability level.

effect, the architecture of the bilayers, built of interdigitated ammonium cations interacting *via* weak C–H... $\pi$  bridges, is preserved in the crystalline state irrespective of the counterion type (Hodorowicz *et al.*, 2005). These properties predispose the ammonium cations to be utilized in the crystal

engineering of layered materials as structure-directing agents (Rey *et al.*, 2004; Shen *et al.*, 2003). On the other hand, the incorporation of organic ions into inorganic frameworks opens the way for the engineering of a new class of layered multifunctional materials.

## Experimental

All chemicals were of reagent grade quality and were obtained from commercial sources and used without further purification. The crystalline phase was obtained using a mixture of aqueous solutions of  $\text{Pb}(\text{NO}_3)_2$  and the ammonium bromide in a 1:2 molar ratio. Well shaped crystals were obtained by slow evaporation at room temperature.

### Crystal data

$(\text{C}_{19}\text{H}_{34}\text{N})[\text{PbBr}_3]$   
 $M_r = 723.39$   
 Monoclinic,  $P2_1/c$   
 $a = 9.4354(1) \text{ \AA}$   
 $b = 34.7040(5) \text{ \AA}$   
 $c = 7.6873(1) \text{ \AA}$   
 $\beta = 92.062(1)^\circ$

$V = 2515.55(6) \text{ \AA}^3$   
 $Z = 4$   
 Mo  $K\alpha$  radiation  
 $\mu = 11.47 \text{ mm}^{-1}$   
 $T = 293 \text{ K}$   
 $0.19 \times 0.06 \times 0.05 \text{ mm}$

### Data collection

Nonius KappaCCD diffractometer  
 Absorption correction: multi-scan  
 (*DENZO* and *SCALEPACK*;  
 Otwinowski & Minor, 1997)  
 $T_{\text{min}} = 0.219$ ,  $T_{\text{max}} = 0.598$

9624 measured reflections  
 6250 independent reflections  
 3604 reflections with  $I > 2\sigma(I)$   
 $R_{\text{int}} = 0.030$

### Refinement

$R[F^2 > 2\sigma(F^2)] = 0.039$   
 $wR(F^2) = 0.076$   
 $S = 1.01$   
 6250 reflections  
 221 parameters

194 restraints  
 H-atom parameters constrained  
 $\Delta\rho_{\text{max}} = 0.67 \text{ e \AA}^{-3}$   
 $\Delta\rho_{\text{min}} = -0.52 \text{ e \AA}^{-3}$

Suitable single crystals of the title compound were carefully selected using a polarizing microscope. The anisotropic atomic

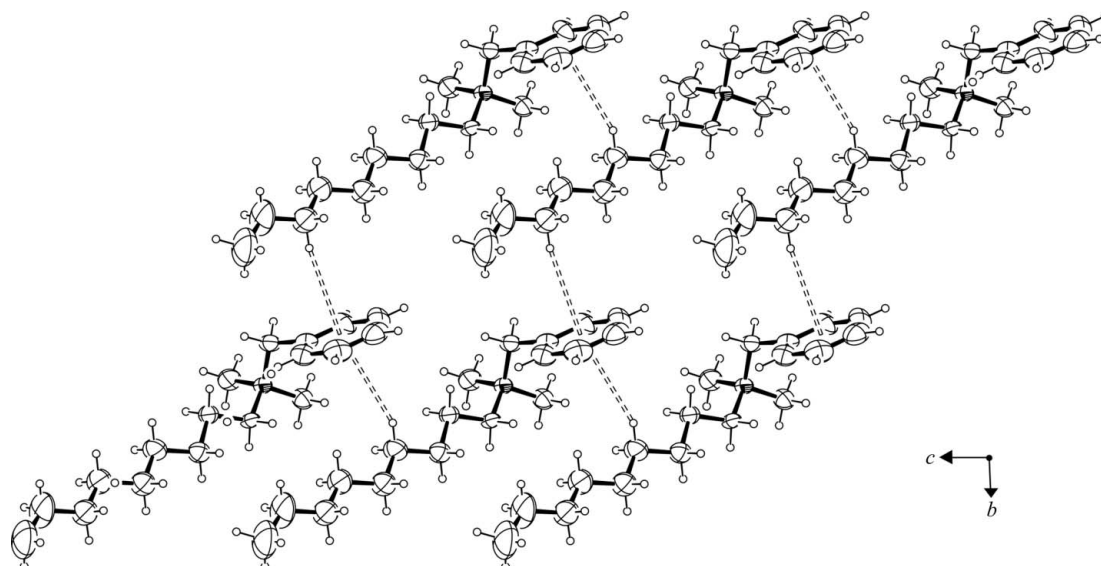


**Figure 5**  
Self-assembly of the ammonium cations in hydrophobic layers, with C13–H...Cg1 and C16–H...Cg1 interactions indicated by dashed lines, where Cg1 is the centroid of the C41–C46 benzene ring. Displacement ellipsoids are shown at the 30% probability level.

**Table 1**

Selected geometric parameters (Å, °).

N1—C2	1.499 (7)	C15—C16	1.381 (10)
N1—C1	1.501 (6)	C16—C17	1.440 (11)
N1—C3	1.502 (7)	C17—C18	1.412 (11)
N1—C4	1.522 (7)	C18—C19	1.360 (12)
C1—C11	1.514 (8)	Pb1—Br4	2.9420 (7)
C4—C41	1.487 (9)	Pb1—Br3	2.9883 (6)
C11—C12	1.505 (8)	Pb1—Br2	3.0106 (6)
C12—C13	1.516 (9)	Pb1—Br2 <sup>i</sup>	3.0504 (6)
C13—C14	1.432 (9)	Pb1—Br3 <sup>i</sup>	3.0627 (6)
C14—C15	1.505 (10)	Pb1—Br4 <sup>ii</sup>	3.1323 (7)
Br4—Pb1—Br3	99.039 (19)	Br2 <sup>i</sup> —Pb1—Br3 <sup>i</sup>	85.365 (17)
Br4—Pb1—Br2	92.014 (19)	Br4—Pb1—Br4 <sup>ii</sup>	174.33 (2)
Br3—Pb1—Br2	87.391 (17)	Br3—Pb1—Br4 <sup>ii</sup>	81.286 (18)
Br4—Pb1—Br2 <sup>i</sup>	84.885 (19)	Br2—Pb1—Br4 <sup>ii</sup>	82.336 (18)
Br3—Pb1—Br2 <sup>i</sup>	173.57 (2)	Br2 <sup>i</sup> —Pb1—Br4 <sup>ii</sup>	95.316 (19)
Br2—Pb1—Br2 <sup>i</sup>	97.60 (2)	Br3 <sup>i</sup> —Pb1—Br4 <sup>ii</sup>	102.460 (18)
Br4—Pb1—Br3 <sup>i</sup>	83.211 (18)	Pb1—Br2—Pb1 <sup>ii</sup>	78.714 (14)
Br3—Pb1—Br3 <sup>i</sup>	90.030 (18)	Pb1—Br3—Pb1 <sup>ii</sup>	78.860 (14)
Br2—Pb1—Br3 <sup>i</sup>	174.16 (2)	Pb1—Br4—Pb1 <sup>i</sup>	78.443 (17)
C2—N1—C1—C11	−59.4 (7)	C11—C12—C13—C14	176.0 (8)
C3—N1—C1—C11	−177.6 (5)	C12—C13—C14—C15	176.3 (8)
C4—N1—C1—C11	62.3 (7)	C13—C14—C15—C16	179.7 (10)
C2—N1—C4—C41	−171.6 (6)	C14—C15—C16—C17	177.1 (10)
C1—N1—C4—C41	65.3 (7)	C15—C16—C17—C18	173.9 (12)
C3—N1—C4—C41	−53.8 (7)	C16—C17—C18—C19	171.1 (13)
N1—C1—C11—C12	176.4 (5)	N1—C4—C41—C46	−86.4 (8)
C1—C11—C12—C13	−176.1 (6)	N1—C4—C41—C42	98.4 (7)

 Symmetry codes: (i)  $x, -y + \frac{3}{2}, z - \frac{1}{2}$ ; (ii)  $x, -y + \frac{3}{2}, z + \frac{1}{2}$ .

displacement parameters of all non-H atoms were restrained using rigid-bond and pseudo-isotropic restraints (DELU 0.01 0.01 and ISOR 0.1 0.2 instructions of *SHELXL97*; Sheldrick, 2008). This was deemed necessary because of the strong absorption of the material and the unmodelled disorder in the organic side chain. H atoms were included from geometrical constraints in a riding model assuming C—H = 0.97 Å for CH<sub>2</sub> groups, 0.96 Å for CH<sub>3</sub> groups and 0.93 Å for aromatic H atoms, and with  $U_{\text{iso}}(\text{H}) = 1.5U_{\text{eq}}(\text{C})$  for methyl groups and  $1.2U_{\text{eq}}(\text{C})$  otherwise.

Data collection: *COLLECT* (Nonius, 1997); cell refinement: *SCALEPACK* (Otwinowski & Minor, 1997); data reduction: *DENZO* (Otwinowski & Minor, 1997) and *SCALEPACK*; program(s) used to solve structure: *SHELXS97* (Sheldrick, 2008); program(s) used to refine structure: *SHELXL97* (Sheldrick, 2008); molecular graphics: *ORTEP-3* (Farrugia, 1997) and *BS* (Ozawa & Kang, 2004); software used to prepare material for publication: *SHELXL97*.

The authors thank the Joint X-ray Laboratory Faculty of Chemistry, and SLAFIBS, Jagiellonian University, for making the Nonius KappaCCD diffractometer available.

Supplementary data for this paper are available from the IUCr electronic archives (Reference: DT3013). Services for accessing these data are described at the back of the journal.

**Table 2**

Hydrogen-bond geometry (Å, °).

Cg1 is the centroid of the C41—C46 benzene ring.

$D-H \cdots A$	$D-H$	$H \cdots A$	$D \cdots A$	$D-H \cdots A$
C11—H11B <sup>iii</sup> ···Br3 <sup>iii</sup>	0.97	3.09	3.761 (7)	128
C3—H3C <sup>iv</sup> ···Br3 <sup>iv</sup>	0.96	3.04	3.950 (7)	159
C2—H2B <sup>iii</sup> ···Br3 <sup>iii</sup>	0.96	3.23	3.992 (7)	137
C4—H4A <sup>v</sup> ···Br4	0.97	2.84	3.757 (6)	159
C1—H1B <sup>v</sup> ···Br4 <sup>v</sup>	0.97	2.98	3.779 (5)	141
C42—H42 <sup>vi</sup> ···Br2	0.93	2.93	3.823 (8)	161
C2—H2C <sup>i</sup> ···Br2 <sup>i</sup>	0.96	2.93	3.837 (7)	159
C2—H2A <sup>ii</sup> ···Br2 <sup>ii</sup>	0.96	3.03	3.788 (7)	137
C3—H3B <sup>iii</sup> ···Br2	0.96	3.17	4.049 (6)	153
C13—H13A <sup>vi</sup> ···Cg1 <sup>vi</sup>	0.97	3.37	3.989	123
C16—H16B <sup>iii</sup> ···Cg1 <sup>iii</sup>	0.97	3.22	3.880	127

 Symmetry codes: (i)  $x, -y + \frac{3}{2}, z - \frac{1}{2}$ ; (iii)  $x - 1, y, z - 1$ ; (iv)  $x - 1, -y + \frac{3}{2}, z - \frac{1}{2}$ ; (v)  $x - 1, y, z$ ; (vi)  $x, y, z - 1$ .

## References

- Billing, D. G. & Lemmerer, A. (2006). *Acta Cryst.* **C62**, m264–m266.
- Bonamartini-Corradi, A., Bruckner, S., Cramarossa, M. R., Manfredini, T., Menabue, L., Saladini, M., Secani, A., Sandrolini, F. & Giusti, J. (1993). *Chem. Mater.* **5**, 90–97.
- Bonamartini-Corradi, A., Cramarossa, M. R., Manfredini, T., Giusti, J., Battaglia, L. P., Saccani, A. & Sandrolini, F. (1994). *Chem. Mater.* **6**, 1499–1503.
- Cheetham, A. K., Rao, C. N. R. & Feller, R. K. (2006). *Chem. Commun.* **46**, 4780–4795.
- Day, P. (1983). *Chem. Br.* **19**, 306–314.
- Elleuch, S., Boughzala, H., Driss, A. & Abid, Y. (2007). *Acta Cryst.* **E63**, m306–m308.
- Farrugia, L. J. (1997). *J. Appl. Cryst.* **30**, 565.
- Hodorowicz, M., Stadnicka, K. & Czapkiewicz, J. (2005). *J. Colloid Interf. Sci.* **290**, 76–82.
- Krautscheid, H., Lode, Ch., Vielsack, F. & Vollmer, H. (2001). *J. Chem. Soc. Dalton Trans.* pp. 1099–1104.
- Kwalek, T., Hodorowicz, M., Stadnicka, K. & Czapkiewicz, J. (2003). *J. Colloid Interf. Sci.* **264**, 14–19.
- Malone, J. F., Murray, C. M., Charlton, M. H., Docherty, R. & Lovery, A. J. (1997). *J. Chem. Soc. Faraday Trans.* **93**, 3429–3436.
- Mitzi, D. B., Chondroudis, K. & Kagan, C. R. (2001). *IBM J. Res. Dev.* **45**, 29–33.
- Nagapetyan, S. S., Dolzhenko, Yu. I., Arakelova, E. R., Koshkin, V., Struchov, Yu. T. & Shklover, V. (1988). *Russ. J. Inorg. Chem.* **33**, 1614–1618.
- Nonius (1997). *COLLECT*. Nonius BV, Delft, The Netherlands.
- Otwinowski, Z. & Minor, W. (1997). *Methods in Enzymology*, Vol. 276, *Macromolecular Crystallography*, Part A, edited by C. W. Carter Jr & R. M. Sweet, pp. 307–326. New York: Academic Press.
- Ozawa, T. C. & Kang, S. J. (2004). *BS (Balls & Sticks)*. URL: <http://www.softbug.com/toycrate/bs>.
- Papavassiliou, G. C. (1997). *Prog. Solid State Chem.* **25**, 125–270.
- Portier, J., Choy, J.-H. & Subramanian, M. A. (2001). *Int. J. Inorg. Mater.* **3**, 581–592.
- Ravindran, M., Willey, R. G. & Drew, M. G. B. (1990). *Inorg. Chim. Acta*, **175**, 99–103.
- Rey, F., Rius, J., Sabater, M. J. & Valencia, S. (2004). *Nature*, **431**, 287–290.
- Shannon, R. D. (1976). *Acta Cryst.* **A32**, 751–767.
- Sheldrick, G. M. (2008). *Acta Cryst.* **A64**, 112–122.
- Shen, S. D., Tian, B. Z., Yu, C. Z., Xie, S., Zhang, Z., Tu, B. & Zhao, D. (2003). *Chem. Mater.* **15**, 4046–4051.
- Willett, R. D. (1991). *Coord. Chem. Rev.* **109**, 181–205.